



OPEN Multiomics approach provides insight into altered choline metabolism and liver injury in patients with glycogen storage disease type Ia

Francesca Pirozzi^{1,9}, Ramin Amiri^{2,9}, Camilla Luni², Alessandro Rossi^{3,4}, Daniela Melis⁵, Roberta Fedele⁶, Carmen Rosano³, Pietro Strisciuglio³, Maaïke H. Oosterveer⁷, Terry G. J. Derks⁴, Giancarlo Parenti^{3,8}, Marianna Caterino^{1,6}✉ & Margherita Ruoppolo^{1,6}✉

Glycogen storage disease type Ia (GSDIa) is an inherited disorder of carbohydrate metabolism. Patients present with excessive storage of glycogen and fat in the liver and kidneys and are potentially at risk of developing long-term complications. Currently, the mainstay of treatment is highly tailored dietary regimens aimed at improving metabolic control. In the present study, to better elucidate the mechanisms potentially involved in the development of long-term complications, a mass spectrometry-based strategy was employed for an in-depth characterization of the serum proteomic and metabolomic profile of n.12 GSDIa patients. The detection of differential abundance of highly liver-specific circulating proteins and choline-related metabolites in patients provides new insights into the extent of liver damage and dysregulation of lipid metabolism in GSDIa. Specifically, the differential abundance of serum aldolase B and its positive correlation with traditional liver function markers supports its role as a potential biomarker for long-term monitoring of GSDIa liver injury.

Keywords Glycogen storage disease type Ia, Multiomics, Lipid metabolism, Liver injury, Serum biomarkers, ALDOB

Abbreviations

ACTA1	Actin, alpha skeletal muscle
ACTG1-ACTB	Actin, cytoplasmic 2
Ala	Alanine
ALDOB	Fructose-bisphosphate aldolase b
APOA5	Apolipoprotein A5
APOC3	Apolipoprotein C3
APOC4	Apolipoprotein C4
APOD	Apolipoprotein D
Asp	Aspartate
beta-Ala	Beta-alanine
BTD	Biotinidase
CDH13	Cadherin-13

¹Department of Molecular Medicine and Medical Biotechnology, University of Naples Federico II, Naples, Italy. ²Department of Civil, Chemical, Environmental and Materials Engineering (DICAM), University of Bologna, Bologna, Italy. ³Section of Pediatrics, Department of Translational Medical Sciences, University of Naples Federico II, Naples, Italy. ⁴Section of Metabolic Diseases, Beatrix Children's Hospital, University Medical Centre Groningen, University of Groningen, Groningen, The Netherlands. ⁵Department of Medicine, Surgery and Dentistry 'Scuola Medica Salernitana', University of Salerno, Salerno, Italy. ⁶CEINGE—Biotecnologie Avanzate Franco Salvatore S.C.A.R.L., Naples, Italy. ⁷Department of Pediatrics and Laboratory Medicine, University Medical Center Groningen, University of Groningen, Groningen, The Netherlands. ⁸Telethon Institute of Genetics and Medicine, Pozzuoli, Italy. ⁹Francesca Pirozzi and Ramin Amiri have contributed equally. ✉email: marianna.caterino@unina.it; margherita.ruoppolo@unina.it

CES1	Liver carboxylesterase 1
CNGDF	Continuous nocturnal gastric drip-feeding
CTSD	Cathepsin D
F10	Coagulation factor X
F11	Coagulation factor XI
FAH	Fumarylacetoacetase
G6P	Glucose-6-phosphate
G6Pase-α	Glucose-6-phosphatase- α
G6Pase complex	Glucose-6-phosphatase complex
Glu	Glutamate
HC	Healthy controls
HCA	Hepatic adenoma
HCC	Hepatic carcinoma
ICAM1	Intercellular adhesion molecule 1
IGLV5-45	Immunoglobulin lambda variable 5-45
Lac	Lactate
MASLD	Metabolic dysfunction-associated steatotic liver disease
MASH	Metabolic dysfunction-associated steatohepatitis
MUC5B	Mucin-5B
PEMT	Phosphatidylethanolamine N-MethylTransferase
PIGR	Polymeric immunoglobulin receptor
PI16	Peptidase inhibitor 16
PRG4	Proteoglycan 4
Pro	Proline
p-Cresol-SO4	P-Cresol sulfate
PZP	Pregnancy zone protein
SAM	S-adenosylmethionine
SHBG	Sex hormone-binding globulin
UCCS	Uncooked corn starch
VCAM	Vascular cell adhesion protein 1
VNN1	Pantetheinase
GSDIa	Glycogen storage disease type Ia

Glycogen storage diseases (GSDs), also referred to as glycogenoses, constitute a group of rare, monogenic disorders caused by defects in glycogen synthesis or glycogen breakdown. These diseases are characterised by abnormal tissue deposition of glycogen¹⁻³. Glycogen storage disease type Ia (GSDIa; OMIM#232200) is caused by inactivating mutations in the G6PC1 gene encoding glucose-6-phosphatase- α (G6Pase- α), the catalytic subunit of the glucose-6-phosphatase complex. G6Pase- α plays a pivotal role in glucose homeostasis by catalysing the hydrolysis of intracellular glucose-6-phosphate (G6P) to glucose and free phosphate in the lumen of the endoplasmic reticulum, in the final step of gluconeogenesis and glycogenolysis^{4,5}. As a result, during periods of fasting, patients with GSDIa experience an inability to release glucose into the bloodstream, resulting in hypoglycaemia⁶. G6P is the first intermediate of intracellular glucose metabolism and plays a central role in hepatic energy metabolism, acting as a metabolic link among glycolysis, the pentose phosphate pathway, glycogen synthesis, de novo lipogenesis and the hexosamine pathway⁷. Consequently, GSDIa patients present a wide range of additional biochemical manifestations, such as hyperlactatemia, hyperlipidaemia, hypertriglyceridemia and hyperuricemia⁸. The tissue expression of G6Pase- α , which is restricted to the liver, kidneys, and, to a lesser extent, the intestine, determines the clinical phenotype of the disease. This primarily results in excessive storage of glycogen and fat in the tissues, leading to hepatomegaly with hepatic steatosis and kidney disease. Despite the recent focus on novel therapeutic approaches in the field^{9,10}, current treatment strategies for GSDIa remain largely symptomatic. The primary treatment strategy for patients with GSDIa involves adherence to a highly personalised dietary regimen comprising frequent feeding, uncooked corn starch (UCCS), and/or continuous nocturnal gastric drip-feeding (CNGDF). This approach has contributed to improvements in prognosis and long-term outcomes in recent decades^{6,8,11}. However, over time, despite good metabolic control, acute hypoglycaemia and complications such as hepatocellular adenomas (HCA), which may progress to hepatocellular carcinoma (HCC)^{8,12,13}, and renal failure^{14,15} may occur. In this regard, elevated levels of circulating lipids have been observed to be a contributing factor. Indeed, an association has been demonstrated between elevated levels of serum triglycerides (TG) in childhood and the risk of developing HCA in patients with GSDIa¹⁶, as well as an association between hyperlipidaemia and the progression of renal damage¹⁷. In the present study, the characterisation of the serum lipidomic profile previously performed in a cohort of patients with GSDIa¹⁸ was complemented by metabolomic and proteomic analysis of the same serum sample from the same patients. This approach provided a more comprehensive and detailed perspective on the metabolic changes associated with GSDIa that cannot be detected by conventional analytical methods. The ultimate goal of this study was to gain further insight into the alterations in lipid metabolism previously observed in GSDIa patients and to expand the investigation to the identification of serum metabolites and/or proteins potentially associated with the disease phenotype. This approach aimed to uncover novel biomarkers linked to GSDIa, which could contribute to a better understanding of the molecular mechanisms underlying the disease and its long-term complications. Given the complexity of the biological system in both health and disease, the added value of our study was a broader and more comprehensive knowledge in the field of GSDIa by integrating data from different molecular levels.

Results

Serum proteomic profile of patients with GSDIa reveals altered liver-specific and lipid metabolism-related proteins

In the present study, a label-free quantitative (LFQ) proteomics approach was employed to investigate the GSDIa serum proteome in a cohort of 12 patients with GSDIa, compared to 12 age- and sex-matched healthy controls (HC). A total of 406 proteins were identified and quantified, and a detailed list of the quantified proteins is provided in the supplementary material (Supplementary Table 1). This includes the UniProtKB/Swiss-Prot ID, gene name, relative quantification in each sample and differential analysis results for each protein. To assess changes in the serum proteome of patients with GSDIa and HC, entire data sets were processed by multivariate and univariate statistical analyses. Firstly, a principal component analysis (PCA) was conducted to estimate the variability between and within each data set. The PCA plot (Fig. 1a) illustrates the distribution of samples along the first two principal components (PC1 and PC2), which explain 18.06% and 11.44% of the total variance in the data, respectively. The plot demonstrates effective clustering between patients and healthy controls (HC), with one patient (P6) borderline between the two conditions. Subsequent to this, a heat map was generated following hierarchical clustering of the most differentially expressed serum proteins for adj. $p < 0.01$ and absolute fold change $|FC| > 2$ between patients and HC (Fig. 1b). Based on these 24 highly differential proteins, the dendrogram structure exhibited clear separation of patients in the two groups, with the exception of patient P6. The complete heat map of differential proteins according to less stringent criteria (adj. $p < 0.05$, $|FC| > 1.5$) is provided in Supplementary Fig. 1a. In order to provide a more comprehensive representation of the serum proteins that exhibited the most significant differential abundance between patients with GSDIa and HC, a volcano plot analysis was employed, based on the relative abundance, expressed as \log_2FC , and statistical significance levels, expressed as $-\log_{10}(p \text{ value})$ (see Fig. 1c and Supplementary Fig. 1b). Specifically, Fig. 1c provides the expression pattern of proteins differential for adj. $p < 0.05$ and $|FC| > 1.5$. Furthermore, the Fig. 1c also provides the labelling of 24 differential proteins for adj. $p < 0.01$ and $|FC| > 2$. Among these, n. 15 were found significantly upregulated proteins (ALDOB, APOA5, APOC3, APOC4, BTG, CES1, CTSD, F10, F11, FAH, ICAM1, MUC5B, PIGR, PRG4, VNN1) and n. 9 were significantly downregulated (ACTA1, ACTG1, APOD, CDH13, IGLV5-45, PI16, PZP, SHBG, VCAM1) in the serum of patients with GSDIa compared to HC. The levels of these differentially abundant proteins in GSDIa patients and HC serum samples were expressed using individual scatter plots (Fig. 1d).

In order to elucidate the pathophysiological mechanisms underlying GSDIa, the set of proteins identified as dysregulated in patients was subjected to further investigation. To this end, an evaluation of tissue gene expression and an assessment of functional enrichment analysis were conducted. This investigation yielded two key results. Firstly, bioinformatic analysis of the tissue gene expression profiles revealed an enrichment of proteins (ALDOB, APOC3, APOC4, APOA5, CTSD, CES1, ACTG1, FAH, VNN1, F11, PRG4 and F10) with predominantly hepatic expression (Fig. 2a). This finding contributed to the identification of the possible association between the altered levels of these proteins found in the patients' serum and an organ-specific dysfunction. A heat map illustrating the tissue transcript expression profile of the differential proteins is shown in Fig. 2a. The yellow/blue colour scale for the transcript-expression-pattern (TPM, Transcripts Per Million) score provides information on both the distribution of transcript levels among tissues and the putative tissue-specific relative expression. To further emphasize this result, liver-specific transcriptomic data were extracted and visualized (Fig. 2b), highlighting the hepatic expression of the proteins included in the heatmap of Fig. 2a. In order to assess the association between the altered serum proteome profile and liver damage in GSDIa, correlation analyses were then performed between the proteins identified by GTEX analysis with liver $TPM > 5$. (ALDOB, APOC3, APOC4, APOA5, CTSD, CES1, ACTG1, FAH, VNN1, F11, PRG4, F10, SHBG, BTG, PIGR, ICAM1, PZP) and traditional biochemical liver monitoring parameters (ALT and AST). Both ALDOB and FAH showed a positive linear correlation with ALT and AST levels; however, ALDOB was selected for further consideration due to its higher liver expression (TPM) compared to FAH (Fig. 2b). Notably, ALDOB showed significant correlations with ALT ($p < 0.001$) (Fig. 2c) and AST ($p < 0.01$) (Fig. 2d) in patients compared to healthy controls. Furthermore, ALDOB levels showed a strong positive correlation with serum uric acid ($p < 0.05$) (Fig. 2e), a parameter commonly used to monitor kidney function and gout risk in GSDIa. Importantly, ALT, AST and uric acid levels were all significantly elevated in patients compared to controls (Fig. 2f–h), supporting the clinical relevance of these findings.

Secondly, a functional enrichment analysis of the differential protein list revealed a significant enrichment of processes primarily related to lipid metabolism using an FDR cutoff of 0.05 and a minimum pathway size of 5. In order to identify specific altered biological processes underlying the GSDIa condition, the Gene Ontology (GO) database was used to analyse the data. The top 10 enriched pathways are shown in Fig. 2i. Consistently with these molecular findings, Fig. 2j reports a plot showing significantly altered levels of total cholesterol from routine clinical biochemistry, highlighting a marked increase in GSDIa patients compared to healthy controls ($p < 0.0001$).

Serum metabolomic profile of patients with GSDIa reveals features consistent with liver dysfunction and dysregulation of lipid metabolism

In the present study, the serum metabolomic profile of patients with GSDIa was obtained by using a targeted liquid chromatography–tandem mass spectrometry (LC–MS/MS)-based approach, which allowed to robustly detect and quantify 73 metabolites. A comprehensive list of the identified and quantified metabolites, including metabolite names, abbreviations, group classifications and their raw concentrations, is provided in Supplementary Table 2. Changes in the serum metabolome of patients with GSDIa and HC were investigated using multivariate and univariate statistical analyses.

To estimate the variability between and within each group of samples, data were analyzed by PCA. With PC1 and PC2 variances of 25.85% and 17.35% respectively, the PCA score plot showed a clear separation between

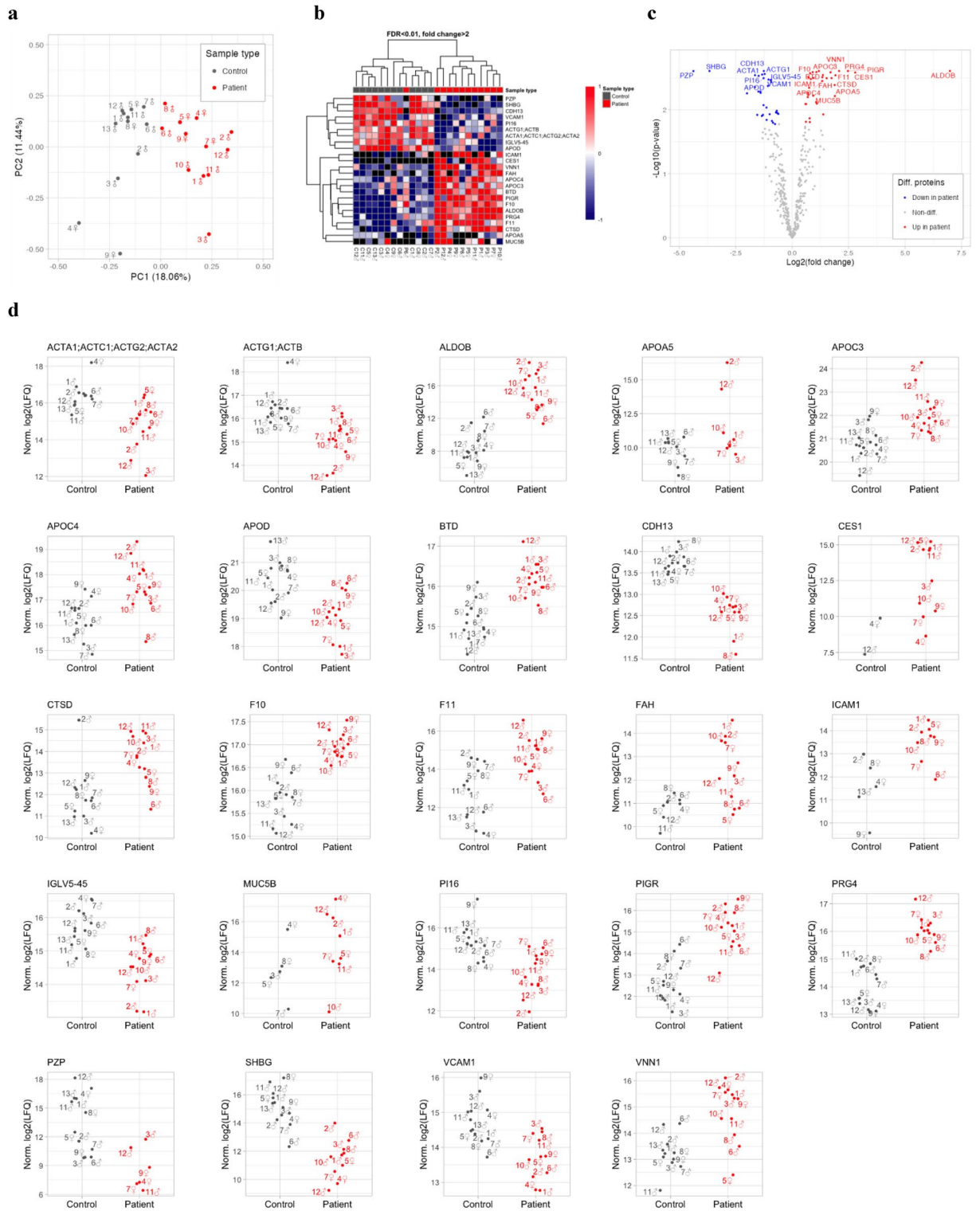


Fig. 1. Serum proteomic profile of patients with GSD1a. **(a)** Principal component analysis (PCA). The first principal component (PC1) explains 18.06% and the second principal component (PC2) explains 11.44% of the total variance in the data between patients and HC. **(b)** Hierarchical clustering with heat map visualization of differential proteins for adj. $p < 0.01$ and $|FC| > 2$. Heat map colour represents relative protein abundance: red and blue represent increased and decreased levels of each protein in patients compared to HC. **(c)** Volcano plot of differential proteins for adj. $p < 0.05$ and $|FC| > 1.5$. Labels only for significantly different proteins with adj. $p < 0.01$ and $|FC| > 2$. Blue and red dots refer to significantly decreased and increased proteins, respectively, in patients compared to HC. **(d)** Scatter plots of all differential proteins with adj. $p < 0.01$ and $|FC| > 2$ in terms of $\log_2(\text{LFQ})$ normalized values. Each dot is annotated with patient number and sex (♂ represents male, ♀ represents female). Missing values, imputed for the differential analysis are not shown. The corresponding tabular data are presented in Supplementary Table 1.

patients with GSDIa and HC along the first PC (Fig. 3a). Metabolites selected as significantly differentially concentrated in sera of patients with respect to HCs were visualized in a heat map after hierarchical clustering (Fig. 3b). With the exception of one healthy control (C6), the dendrogram structure showed clear clustering of the two patient groups. The results of the differential analysis are reported in Supplementary Table 2, and significantly abundant metabolites (adj. $p < 0.01$, $|FC| > 1.5$) were also shown using a volcano plot to highlight significance as a function of relative abundance of each metabolite, expressed as $-\log_{10}(p \text{ value})$ and \log_2 fold change, respectively (Fig. 3c). The analysis identified 14 out of 73 metabolites as differentially abundant between the serum samples of the two study groups. More specifically, patients with GSDIa showed higher levels of beta-Ala, carnosine, choline, Glu, Ala, Asp, Pro, lactate (Lac), sarcosine, serotonin, xanthine, and lower levels of p-cresol-SO₄, Phenylalanine betaine and Trimethylamine N-oxide (TMAO), compared to HC. The \log_2 -transformed concentrations of the significantly differentially abundant metabolites are presented as scatter plots in Fig. 3d. Among these, the altered levels of choline, sarcosine, and TMAO—metabolites intricately linked to phospholipid synthesis and lipoprotein metabolism—point to a potential dysregulation of lipid metabolic pathways in GSDIa patients. Moreover, correlation analyses were conducted in order to explore potential associations between amino acids abundance in patients and their circulating levels of ALT and AST. Specifically, significant positive linear correlations were found between serum levels of Ala and ALT ($p < 0.05$), Ala and AST ($p < 0.01$), Asp and ALT ($p < 0.01$), Asp and AST ($p < 0.001$), Glu and ALT ($p < 0.05$) and Glu and AST ($p < 0.05$) (Fig. 4a–f). These findings suggest a strong link between elevated levels of these amino acids and traditional liver function parameters.

Multiomics data integration provides new insights into relationships gained and lost in disease

To highlight pairs of features that could be directly or indirectly functionally related or take part in common biological processes, Pearson's correlation coefficients were calculated for each protein–protein, metabolite–metabolite, and protein–metabolite pair. Correlations were calculated separately for GSDIa patients and HCs and considered significant with an adjusted p value < 0.1 . All significant correlations in either HCs or patients are shown in Supplementary Fig. 2a, b, respectively, and in Supplementary Table 3. Furthermore, to systematically investigate the role of GSDIa disease on these correlations, those gained or lost under pathologic conditions were reported in Supplementary Fig. 2c and Supplementary Table 3, and the most significant gained or lost correlations were sub-selected and shown in Fig. 5.

In HC serum samples, 180 significant correlations were found (Supplementary Fig. 2a), and, out of these, only 12 were multiomic (between a protein and a metabolite). In particular, negative correlations were found between SHBG and Asparagine, Leucine, Isoleucine, and Lysine, between Desmocollin 1 (DSC1) and Symmetric dimethylarginine, between Superoxide Dismutase 3 (SOD3) and Tryptophan betaine, between Suprabasin (SBSN) and Serotonin, and between Immunoglobulin Lambda Variable 4-69 (IGLV4-69) and Dehydroepiandrosterone sulfate. Positive correlations were found between CBP2 (a.k.a. SERPINH1) and α -, β -, and γ -Aminobutyric acid, and between Complement Factor H Related 3 (CFHR3) and Tryptophan betaine. All these multiomic correlations in HC samples were lost in GSDIa samples (Supplementary Fig. 2c). For GSDIa patient serum samples, 140 significant correlations were found (Supplementary Fig. 2b), with only 3 of these being multiomic: between Alpha-1-Microglobulin/Bikunin Precursor (AMBIP) and Aspartate, between endoplasmic reticulum chaperone BiP (HSPA5) and Homoarginine, and between complement factor H-related protein 2 (CFHR2) and Lactic acid, which were all negative correlations and not significant in HC samples (“gained correlations” in Supplementary Fig. 2c).

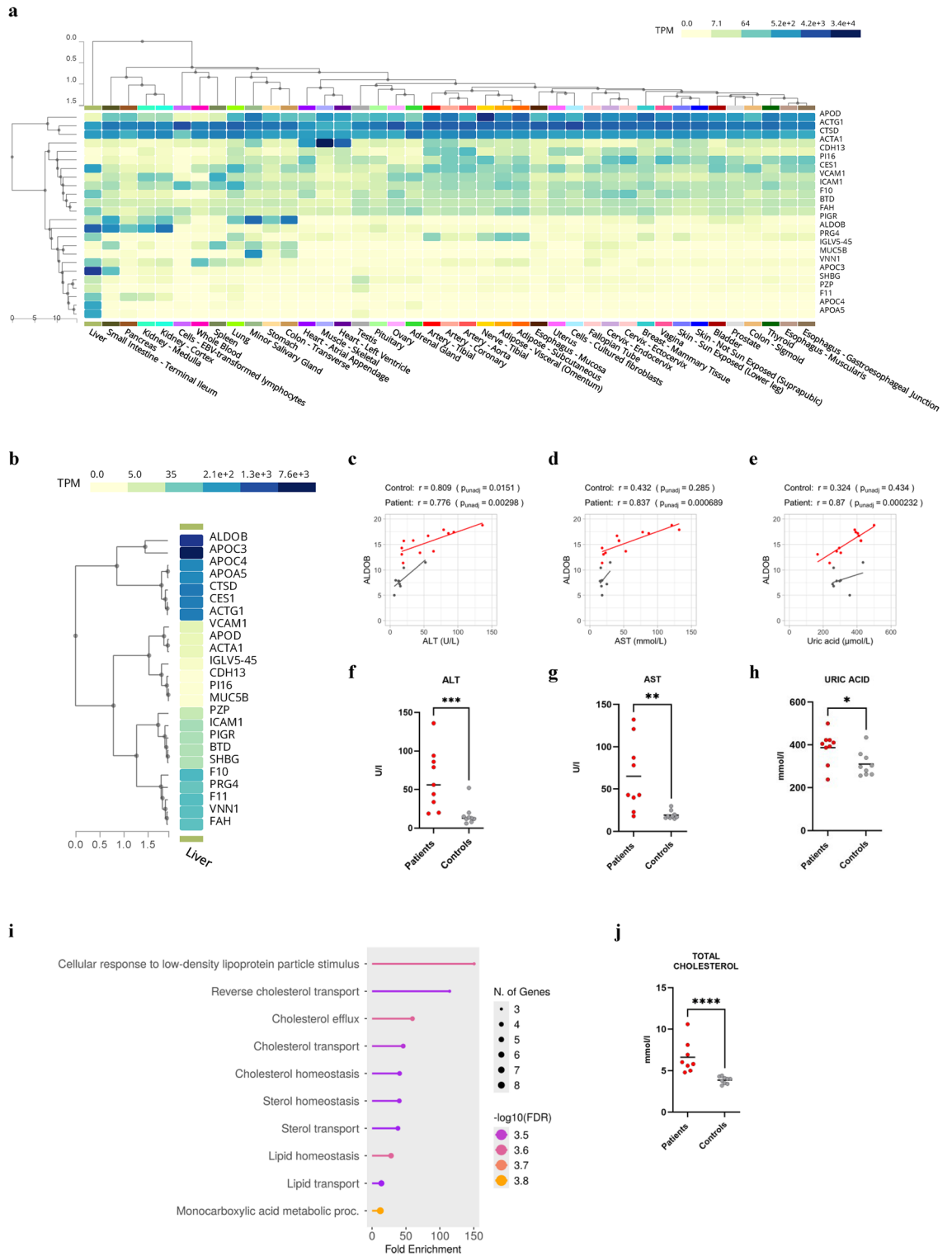
Discussion

The life expectancy of patients with GSDIa has increased significantly over the past decades as a result of advances in dietary management¹¹. Nevertheless, despite the evidence indicating that good metabolic control plays a role in preventing complications in GSDIa¹⁹, acute and chronic complications still occur in patients despite adherence to dietary therapy⁸. In this study, a broad metabolomic approach was applied with the aim of identifying additional metabolic disruptions and gaining deeper insights into the systemic biochemical imbalances associated with GSDIa. Serum samples from 12 patients with GSDIa and sex- and age-matched healthy controls were analyzed. The metabolomic and proteomic serum profiles of GSDIa patients were characterised, allowing a detailed assessment of disease-related molecular alterations.

The characterization of the serum proteomic profile in patients with GSDIa enabled the identification and quantification of 406 proteins. Among these, 24 were found to be significantly dysregulated compared to healthy controls. Enrichment analysis of these differentially expressed proteins revealed two main features. First, a strong involvement in lipid metabolism emerged, consistent with previous findings from our earlier study¹⁸ which characterised the serum lipidomic profile of the same cohort of GSDIa patients analysed here. Second, a predominant liver-specific expression pattern was observed, further supporting the central role of hepatic dysfunction in the molecular landscape of the disease.

Moreover, the results of the present study are consistent with the presence of liver damage in GSDIa. In this regard, a more detailed examination of the literature revealed that the dysregulated proteins identified in the serum of patients with GSDIa overlap with the alteration profile observed in the context of liver disease. This finding underscores the potential for shared mechanisms underlying GSDIa and liver disease. In particular, it has been reported that the levels of eight serum proteins (ALDOB, PIGR, SHBG, APOD, PRG4, APOB, PZP and IGLV5-45) vary in individuals with liver diseases other than GSDIa.

Among these, ALDOB, the hepatic isozyme of fructose-bisphosphate aldolase (EC 4.1.2.13), and PIGR, an immunoglobulin receptor involved in the transcytosis of IgA and IgM, have recently been proposed as potential circulating biomarkers of metabolic dysfunction-associated steatotic liver disease (MASLD) in humans²⁰.



Specifically, both ALDOB and PIGR have been found to be dysregulated in liver diseases, including MASLD, metabolic dysfunction-associated steatohepatitis(MASH) and alcohol-related liver disease (ALD). In detail, ALDOB was found to be up-regulated in plasma from both patients and a mouse model of MASLD²¹, in plasma from individuals with MASH²², in serum from patients with acute and chronic hepatitis²³, and simultaneously up- and downregulated in plasma and liver from individuals with ALD²⁴. PIGR was found to be upregulated in the plasma of both patients with MASLD^{21,25} and a mouse model of MASLD²¹, in the liver and plasma of patients with ALD²⁴, and in the plasma of patients with MASH²² and MASH rat model²⁶. Moreover, ALDOB was found to be upregulated in both the plasma and liver of ob/ob mice, a leptin-deficient model of obesity, whereas PIGR was only upregulated in their plasma²⁷. It is noteworthy that, in accordance with the findings of this study, ALDOB was also identified as being upregulated in the livers of two distinct GSDIa mouse models^{28,29}. In the present study, in alignment with the findings of ALDOB in the context of liver disease, we found

◀ **Fig. 2.** Investigation of differential serum protein content of patients with GSDIa. **(a)** Heatmap of tissue gene expression profile of differential proteins in GSDIa. Heatmap color coding represents different transcript distribution values in different tissues, expressed as TPM. Clustering of liver proteins was observed. **(b)** Extrapolation of liver-specific tissue gene expression profile from **(a)**. **(c–e)** Simple linear regression analysis between $\log_2(\text{LFQ})$ normalized ALDOB values and serum levels of ALT **(c)** and AST **(d)**, and uric acid I in patients with GSDIa. Solid lines represent the result of the linear fit. Solid line colour code represents patient (red) and HC (grey) trend. R: Pearson's correlation. P_{unadj} : uncorrected p value. Missing values, imputed for the differential analysis are not shown. **(f–h)** Plots of differential serum ALT **(f)**, AST **(g)**, and uric acid **(h)** levels, expressed as (means \pm SEM) in GSDIa patients versus HC. The significant difference ($*p < 0.05$, $**p < 0.01$, $***p < 0.001$) was evaluated by performing Mann–Whitney comparison test. **(i)** Lollipop charts of the top 10 biological processes enriched from the input data list of differentially expressed proteins in the serum of patients with GSDIa. The $-\log_{10}(\text{FDR})$ values for each pathway were expressed on a color scale between orange and purple. **(j)** Plot of differential serum total cholesterol levels, expressed as (means \pm SEM) in GSDIa patients versus HC. The significant difference ($*p < 0.05$, $**p < 0.01$, $***p < 0.001$) was evaluated by performing Mann–Whitney comparison test.

a linear positive correlation between circulating ALDOB levels and the transaminases AST and ALT, which are traditional biochemical parameters of liver function; furthermore, consistent with ALDOB implication in de novo lipogenesis in MASLD³⁰, we also found a positive correlation between ALDOB and the fructose-related metabolite uric acid (Fig. 2e), suggesting increased fructose metabolism in GSDIa to provide precursor for gluconeogenesis and de novo lipogenesis. Our previous work demonstrated a specific altered serum lipid signature in the same cohort of patients¹⁸.

Similarly to ALDOB and PIGR, there is evidence to suggest that also the sex hormone binding globulin (SHBG), which was found to be downregulated in GSDIa patients in the present study and in Simons et al.³¹, may also play a role in the pathophysiology of MASLD. In more detail, retrospective and prospective studies of very large cohorts of patients with MASLD^{32,33}, have associated serum levels of SHBG with the development and regression of MASLD, suggesting that SHBG is a new promising biomarker of MASLD. Indeed, SHBG is recognized as a hepatokine and a reliable marker of MASLD, as well as other conditions, including obesity, diabetes mellitus, and insulin resistance³⁴. SHBG is a homodimeric glycoprotein, produced by hepatocytes and secreted into the blood, where it binds with high affinity to circulating sex steroid hormones, and regulates their bioavailability³⁵. In this regard, the dysregulation of SHBG and the demonstration of an inverse correlation between SHBG and the saturated fatty acids fraction and the intrahepatic lipid content in individuals with GSDIa³¹, provide evidence supporting the hypothesis that there is a link between metabolic imbalance in GSDIa and the circulating sex hormone levels in GSDIa which has recently been the subject of increased attention³⁶. Indeed, additional features, including delayed puberty, hypogonadotropic hypogonadism and polycystic ovaries are documented in GSDIa³⁶. In regard to this topic, the findings of a comprehensive systematic review³⁷ and a meta-analysis indicate a correlation between reduced SHBG levels and the presence of polycystic ovary syndrome³⁸. It is noteworthy that, although dietary influence on growth and sexual development is evident, the imbalance in circulating levels of insulin and cortisol observed in hepatic GSDs, whether secondary to dietary treatment or to the enzyme defect, may play a pivotal role in this sense^{36,39}. Indeed, chronic recurrent elevations of cortisol in response to hypoglycemia may lead to the suppression of gonadotropin-releasing hormone (GnRH), luteinizing hormone (LH), and follicle-stimulating hormone (FSH) release, with implications for SHBG biosynthesis³⁶.

It should be noted that the present study found differentially abundant proteins in the serum of patients with GSDIa, including polymeric immunoglobulin receptor (PIGR), proteoglycan 4 (PRG4), pregnancy zone protein (PZP) and immunoglobulin lambda variable 5-45 (IGLV5-45). These proteins may also be relevant in the context of liver disease. These have been linked to HCC studies, and are joined by the previously discussed ALDOB protein. In particular, ALDOB has been identified as a potential prognostic biomarker for overall survival in HCC in a recent study using big data analysis⁴⁰. PIGR, which was found to be upregulated in the serum of patients with GSDIa in the current study, is also being investigated for its ability to exert oncogenic functions through the activation of the ribosomal pathway in HCC⁴¹ and metastasis⁴². PRG4 is a secreted proteoglycan protein predominantly expressed by chondrocytes, which lubricate and protect the surfaces of articular cartilage⁴³. Its mRNA expression in liver cancer tissue was recently shown to correlate with longer survival in HCC patients likely due to its ability to impair HCC cell migration and act as a tumor suppressor in tumors expressing the major PGR4 receptor, CD44⁴⁴. In the case of PZP, an estrogen-related protein that normally increases during pregnancy, there is evidence that its downregulation in HCC tissue may be associated with immune infiltrates and poor prognosis⁴⁵. Furthermore, IGLV5-45, the fifth region of the variable domain of immunoglobulin lambda light chains, which was found to be downregulated in our patients, was found to be upregulated in study of immunodeficiency herpes virus/hepatitis B co-infected patients with HCC⁴⁶.

This study identified differentially abundant proteins in the serum of patients with GSDIa, suggesting possible liver damage, as supported by the aforementioned considerations. Further analysis revealed that some of these differentially abundant proteins have a role in lipid metabolism, which is consistent with our previous lipidomic studies in the same cohort of patients¹⁸. Proteins that are differentially abundant in patients with GSDIa and implicated in lipid metabolism include APOD, APOA5, APOC3, APOC4, BTB, CES1, VNN1, and the above discussed SHBG, PIGR, PRG4, and ALDOB.

Specifically, APOA5, APOC3, APOC4, BTB, VNN1, ALDOB and PIGR were all found to be upregulated in the plasma proteome of ob/ob mice, whereas ALDOB, APOA5 and VNN1 were also found to be upregulated in

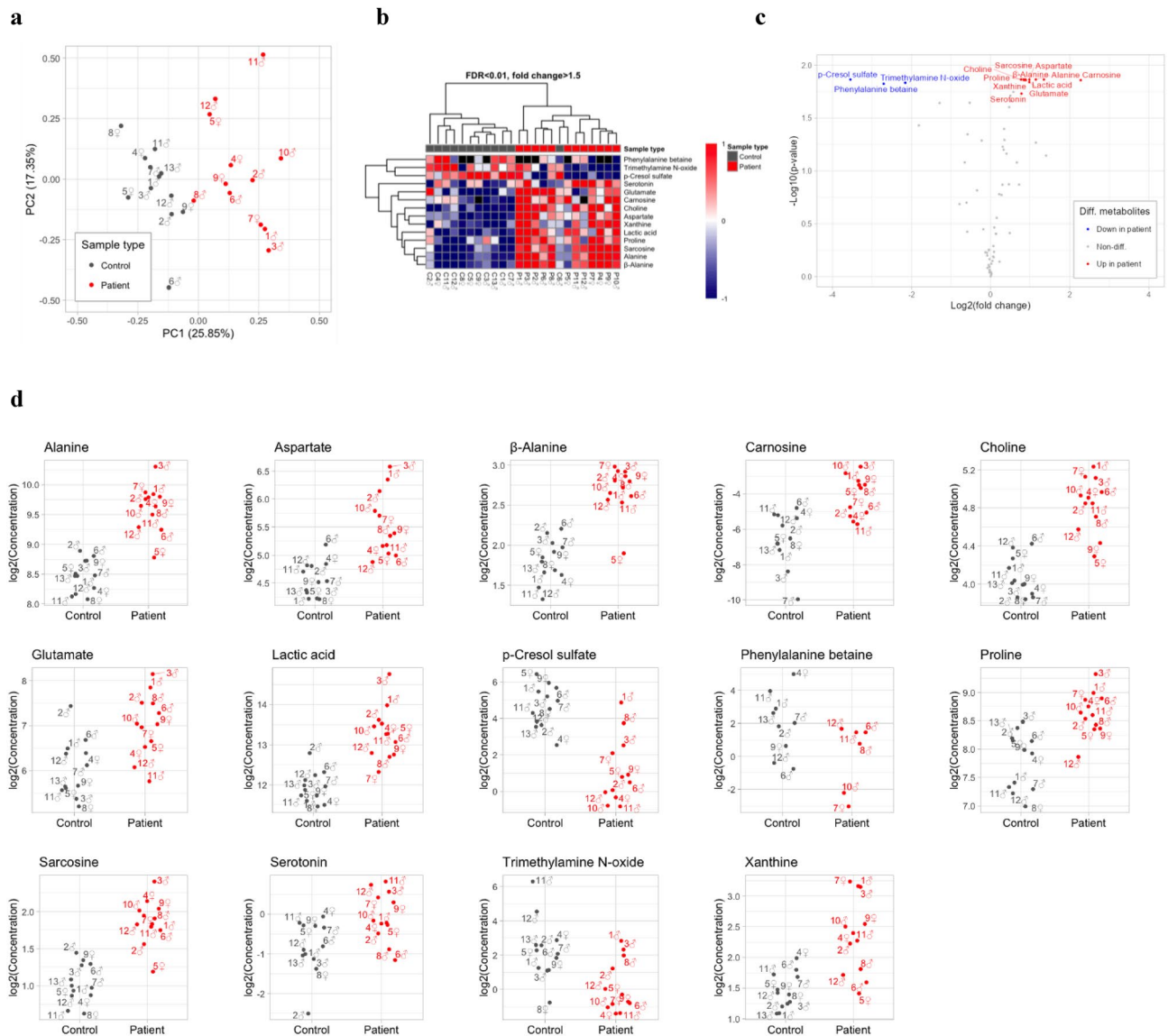


Fig. 3. Serum metabolomics profile of patients with GSD1a. **(a)** Principal component analysis (PCA). The first principal component (PC1) explains 25.85% and the second principal component (PC2) explains 17.35% of the total variance in the data between patients and HC. **(b)** Hierarchical clustering with heat map visualization of differential metabolites for adj. $p < 0.01$ and $|FC| > 1.5$. Heat map colour coding represents relative metabolite abundance: red and blue represent increased and decreased levels of each metabolite in patients compared to HC. **(c)** Volcano plot of differential metabolites for adj. $p < 0.01$ and $|FC| > 1.5$. Blue and red dots refer to significantly decreased and increased metabolites, respectively, in patients compared to HC. **(d)** Scatter plots of the significantly differential metabolites in terms of \log_2 raw concentration. Missing values, imputed for the differential analysis are not shown. The corresponding tabular data are presented in Supplementary Table 2.

both plasma and liver²⁷. In particular, the alterations observed in the apolipoproteins (APOD, APOA5, APOC3, and APOC4), in conjunction with those in the cholesteryl ester hydrolase (CES1), which is predominantly expressed in the liver⁴⁷, provide robust evidence for lipid metabolism disturbances in GSD1a, as corroborated by the lipidomics results¹⁸. With regard to APOD, which was identified as being downregulated in the present study in GSD1a, it has been demonstrated that it is predominantly present in high-density lipoproteins (HDL) and capable of promoting VLDL catabolism⁴⁸. In particular, increased APOD production has been demonstrated to significantly reduce plasma TG levels in mice⁴⁸, while its deficiency has been shown to result in elevated serum TG and insulin levels in mice⁴⁹. The downregulation of APOD in our patients is therefore consistent with these findings and with the results of an altered serum lipidome profile in patients with GSD1a¹⁸ and delayed very-low-density lipoprotein catabolism in GSD1a^{50,51}. Finally, also biotinidase (BTD) and PRG4 seem to be implicated in lipid and glucose metabolism perturbations. In detail and consistent with BTD result obtained, BTD has been proposed as a potential marker of perturbed glucose and lipid metabolism in GSDs^{2,52,53}. In line with the overabundance of PRG4 found in the serum of GSD1a patients in this study and the metabolic disturbances

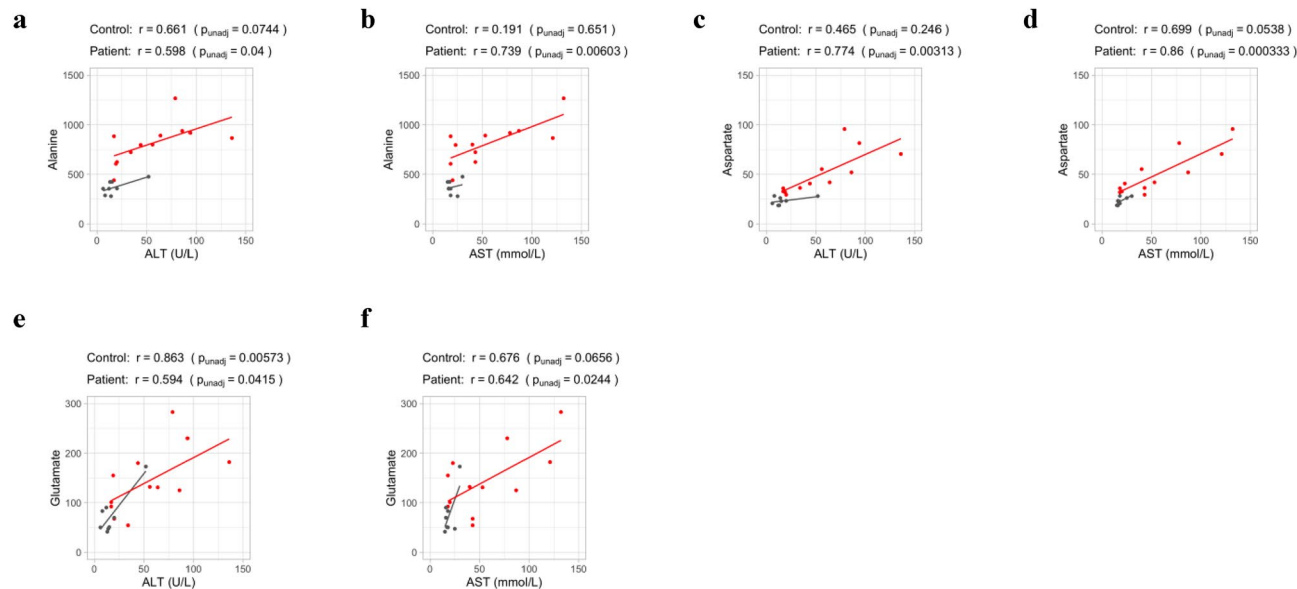


Fig. 4. Relevant clinical correlations between differential serum metabolites and traditional parameters of liver function in GSDIa patients. (a–f) Simple linear regression plots of significant correlations found between differential serum Ala, Asp, Glu levels and serum ALT, AST levels in patients with GSDIa. Solid lines represent the result of the linear fit. Solid line colour code represents patient (red) and HC (grey) trend. R: Pearson's correlation. P_{unadj} : uncorrected p value. Missing values, imputed for the differential analysis are not shown.

typical of GSDIa discussed, it has recently been suggested that PRG4 contributes to weight gain, dyslipidaemia, and insulin resistance⁴³.

The characterization of the serum metabolomic profile of patients with GSDIa allowed the identification and quantification of 73 metabolites out of a total of 80 present in the targeted metabolomics panel. The application of univariate and multivariate statistical analysis revealed differential abundance of 14 metabolites in the serum of patients. In particular, patients with GSDIa exhibited elevated levels of beta-Ala, carnosine, choline, Glu, Ala, Asp, Pro, Lac, sarcosine, serotonin, xanthine, and diminished levels of p-cresol-SO, Phenylalanine betaine and TMAO in comparison to HC. The elevated serum concentrations of Lac are indicative of the hyperlactatemia observed in patients with GSDIa. This condition is believed to arise from an augmented intracellular glycolytic rate, driven by the accumulation of G6P, as previously suggested⁵⁴. With regard to the levels of Glu, Ala, Asp, and Pro found in patients, these amino acids can act as gluconeogenic amino acids in a variety of processes involving transamination to pyruvate (Ala) and through shunting into the TCA cycle by transamination to α -ketoglutarate (Glu), to oxaloacetate (Asp), and by catabolism to α -ketoglutarate (Pro). In particular, transamination reactions are catalysed by ALT and AST, whose serum levels appear to be elevated in patients included in this study. Furthermore, linear positive correlations were identified between serum ALT and Ala, Glu, and Asp, as well as between serum AST and Asp and Ala. These findings indicate a robust correlation between these amino acids and aminotransferase levels. In particular, the comparison with HC revealed a greater and more significant difference in ALT levels than in AST levels. As ALT assays measure the combined activity of both ALT1 and ALT2 isoenzymes, and since ALT1 is predominantly liver-specific⁵⁵, the elevated ALT levels observed likely reflect liver damage in patients with GSDIa. It is noteworthy that serum concentrations of AST and ALT are elevated in GSDIa at the time of diagnosis and often return to normal or near-normal levels with appropriate treatment⁸. Nevertheless, and despite good compliance with dietary treatment, our results show elevated circulating AST and ALT levels in patients with GSDIa, in line with the findings of Farah et al⁵⁶ and Rossi et al⁵⁴ in patients with GSDIa. These results provide further evidence that dietary intervention alone is not sufficient to prevent liver damage.

To provide a more detailed explanation, elevated serum levels of Ala and Asp, when considered as products of transamination reactions, may indicate an increased glycolytic rate (associated with elevated pyruvate levels) and TCA cycle rate (associated with elevated oxaloacetate levels) or an increased need for transport to the liver to supply the gluconeogenic pathway. In particular, there are findings^{54,56} indicating the presence of an increased glycolytic rate and TCA cycle overload in patients with GSDIa. In sum, it can be speculated that in patients with GSDIa, despite optimal glycemic control, there is a positive regulation of gluconeogenesis by both TCA cycle overload (mediated by Asp, Glu, and Pro) and transamination to pyruvate (mediated by Ala) in response to subclinical hypoglycemia. It should also be noted that, in line with data suggesting TCA overload in patients^{54,57}, higher levels of fumarylacetoacetase (FAH) were detected by serum proteomics in patients with GSDIa in the present study.

The elevated serum concentrations of xanthine observed in this study are consistent with the untargeted plasma metabolomics analysis conducted by Mathis et al.⁵⁶ in 14 patients with GSDI, including 11 with GSDIa. This corroborates the hypothesis of altered purine metabolism in GSDIa⁵⁶.

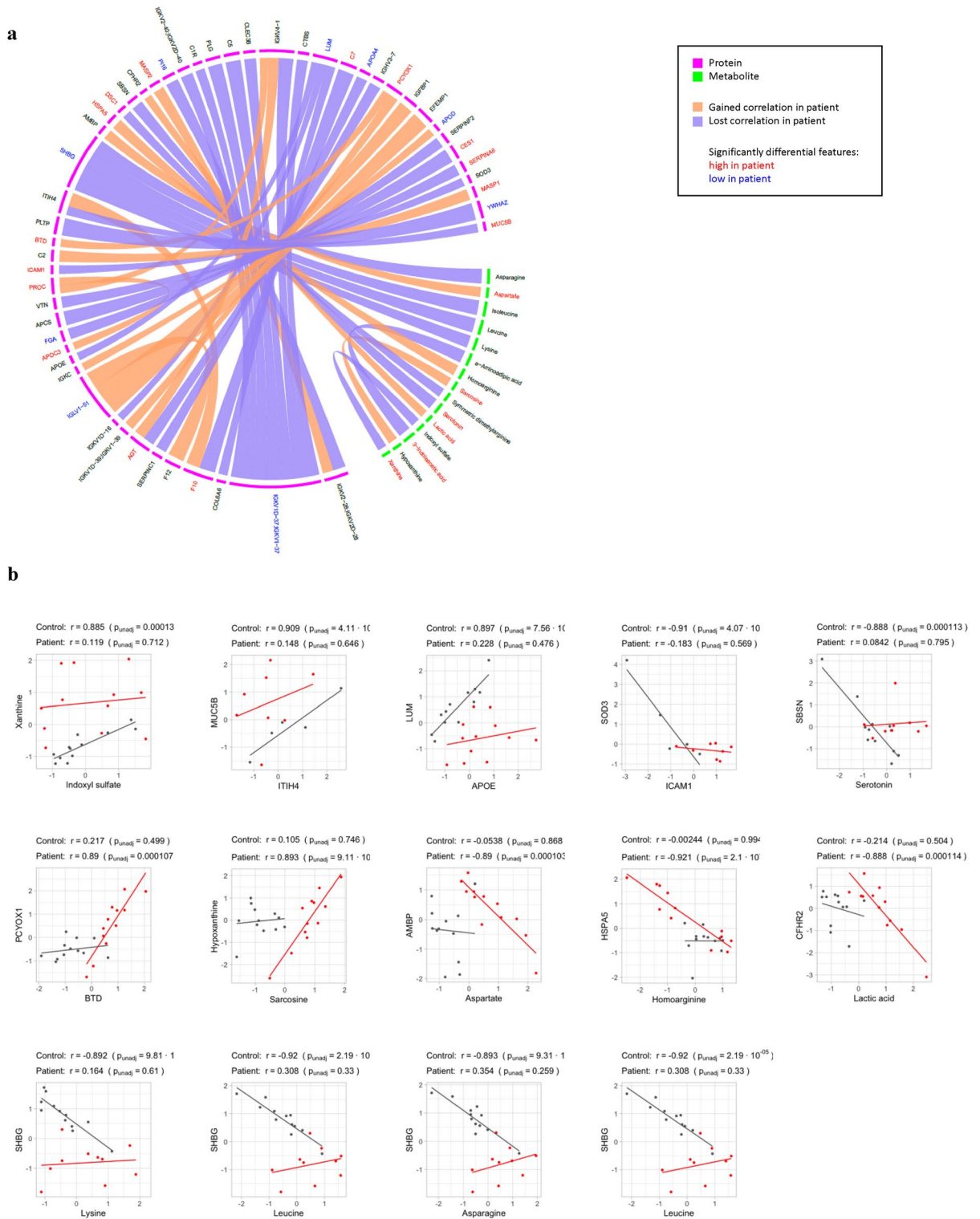


Fig. 5. Multiomics correlation changes in GSD1a. **(a)** Selected lost or gained significant Pearson's correlations in patients with respect to HCs (adjusted p -value < 0.1) with $|\text{corr.coeff patient} - \text{corr.coeff. HC}| > 0.6$ and at least one of the connected features significantly different between patients and HCs. Pink circular sectors correspond to proteins, green to metabolites. The width of the circular sectors is proportional to $|\text{corr. Coeff. Patient} - \text{corr. Coeff. HC}|$. The orange and purple edge colours indicate gained and lost correlations in patients. Molecules highlighted in red are significantly increased in patients, those highlighted in blue are decreased. **(b)** Scatter plot of z-scores of the indicated features with significant correlation difference between control and patient. Solid lines represent the result of the linear fit. Solid line colour code represents patient (red) and HC (grey) trend. R: Pearson's correlation. P_{unadj} : uncorrected p value. Missing values, imputed for the differential analysis are not shown.

Furthermore, the present metabolomic study revealed an elevation in serum choline and sarcosine levels, alongside a pronounced reduction in TMAO, in patients with GSDIa in comparison to HC. Choline is an essential biological molecule for all cells, required for the synthesis of phosphatidylcholine (PC), a structural component of VLDL^{58,59}. PCs participate in the SM cycle and play a key role in the ceramide (Cer) /sphingomyelin (SM) balance, through the hydrolysis of SM by sphingomyelinase and the transfer of phosphocholine from PC to Cer by sphingomyelin synthase⁶⁰. In addition, Choline is also a source of labile methyl groups in the metabolism of homocysteine, through the conversion to betaine⁶¹. In accordance with this, the present study identified elevated serum concentrations of sarcosine and TMAO, two choline-related metabolites, and carnosine (and its precursor, beta-Ala). Carnosine is involved in the reaction catalysed by carnosine N-methyltransferase to produce anserine and S-adenosyl-homocysteine. Sarcosine is one of the choline-related metabolites⁶². Specifically, sarcosine is derived from choline through a series of chemical reactions, including the oxidation of choline to form betaine. Subsequently, betaine undergoes conversion to dimethylglycine, which in turn is converted to sarcosine. TMAO is a choline-related metabolite, resulting from the oxidation of trimethylamine by flavin monooxygenase 3 in the liver. A reduction in TMAO may be indicative of alterations in choline metabolism and dysbiosis of the microbiota in patients with GSDIa, as demonstrated recently⁶³. The findings of the present study have been used to construct a working model of a pathomechanism affecting choline metabolism in GSDIa (Fig. 6). This model integrates the current metabolomic results with the results of our previous study on lipidomics¹⁸. The present study hypothesises that an increase in hepatic choline metabolism in patients with GSDIa supports the increase in PC levels in patients via the Kennedy pathway. This increase, in turn, is hypothesised to support an increase in the SM rate and Lands cycle. Indeed, in our previous study¹⁸ we demonstrated an increase in PC, DG, SM, CER, and LysoPC serum levels in the same cohort of patients with GSDIa.

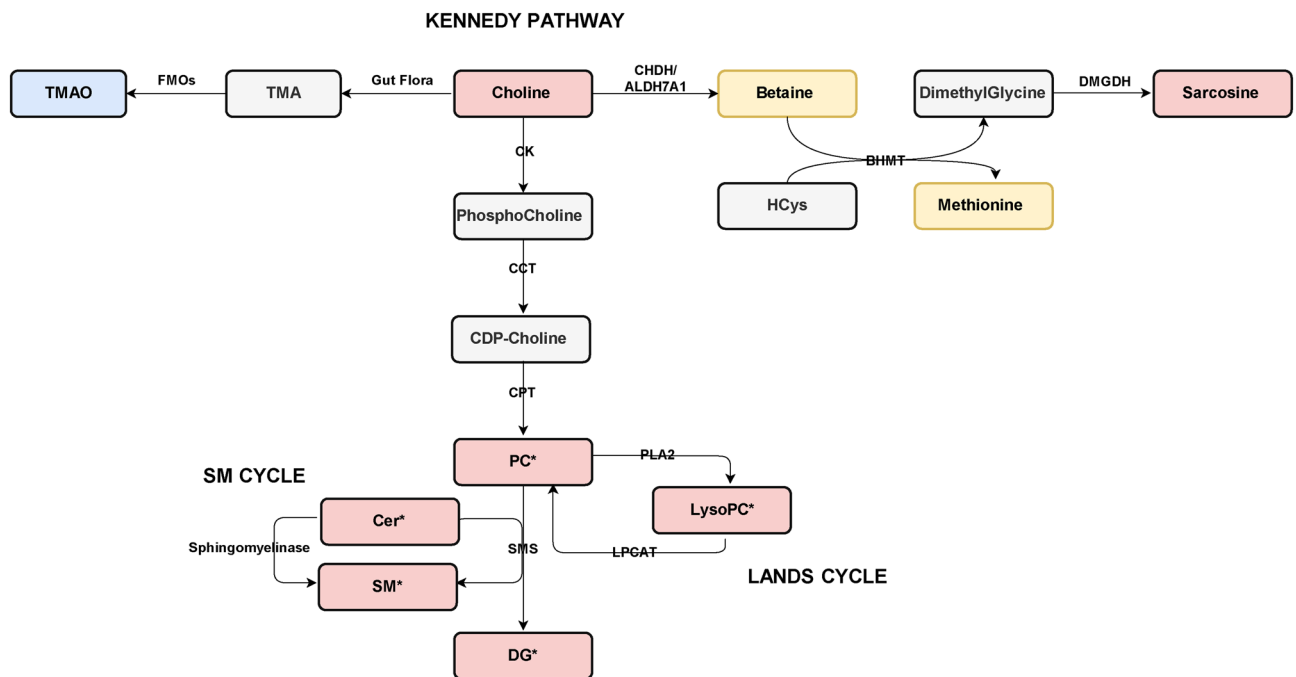


Fig. 6. Proposed pathomechanisms involving choline metabolism in GSDIa. The increase in choline and the decrease in the choline-related metabolite TMAO, in parallel with an increase in the choline-related metabolite sarcosine, and the higher levels of PC, LysoPC, DG, SM and Cer obtained in our previous serum lipidomics study on the same cohort of patients with GSDIa, suggest an increased rate of the Kennedy pathway and, simultaneously, of the SM and Lands cycles in GSDIa. In this context, the role of PC in the Cer/SM balance is crucial: phosphocholine is transferred from PC to Cer via SMS and subsequently released as diacylglycerols. This process is coupled to the hydrolysis of SM to Cer by sphingomyelinase. In addition, PC promotes the increase of LysoPC in the Lands cycle through its hydrolysis mediated by PLA2. Choline is also a methyl group donor in homocysteine metabolism through its conversion to betaine and its metabolism to dimethylglycine. The increase in serum sarcosine levels from dimethylglycine can be explained as compensation for the increased levels of choline converted to PC in the Kennedy pathway. Metabolites detected and identified as elevated are shown in red; those detected and identified as decreased are shown in blue. The presence of an asterisk refers to metabolites that were found to be differentially abundant in our previous lipidomics study¹⁸ performed on the same cohort of GSDIa patients. Metabolites that were measured and found not to be differentially abundant are indicated by a yellow colouring. Abbreviations. ALDH7A1, betaine aldehyde dehydrogenase; BHMT, betaine-homocysteine S-methyltransferase; CCT, phosphocholine cytidylyltransferase; CHDH, choline dehydrogenase; CK, choline kinase; CPT, cholinephosphotransferase; DMGDH, dimethylglycine dehydrogenase; FMOs, flavin monooxygenase enzymes; LPCAT, Lysophosphatidylcholine acyltransferase; PLA2, Phospholipase A2; SMS, sphingomyelin synthase.

The following study assessed, through a multi-omics approach, potential correlations between metabolites and proteins in order to identify meaningful associations related to the disease. This strategy allowed the identification of molecular relationships that may arise from shared pathophysiological mechanisms, even without a direct link. It is important to note that correlation does not imply causation. For instance, two features may appear correlated because they are both indirectly influenced by a third factor, rather than being directly related to each other. There is no direct evidence in the literature linking many of the identified correlated features and follow-up research is required to unravel the underlying mechanisms. Nevertheless, correlation analysis—both at the single- and multi-omics levels—can help identify disease-associated processes, even when the molecules involved are differently affected, as observed in the case of sarcosine and hypoxanthine. The present study revealed a significant increase in serum sarcosine concentration in patients, whereas hypoxanthine levels did not differ between groups. However, patient samples exhibited a higher concentration of xanthine (a metabolite of hypoxanthine) than HC subjects. As previously discussed, sarcosine is a secondary metabolite of choline, an important component of hepatic lipid metabolism, and xanthine oxidase, the enzyme responsible for the oxidation of hypoxanthine to xanthine and subsequently to uric acid, is predominantly expressed in the liver. Consequently, these observations imply that the observed correlation between sarcosine and hypoxanthine may be attributable to the concomitant presence of altered (albeit distinct) processes associated with liver disease. It is noteworthy that this positive relationship between sarcosine and hypoxanthine is only observed in the context of the disease; in HCs, no discernible relationship between these two molecules is observed. This observation can be attributed to the disease-specific nature of this relationship.

Limitations of the study

Despite the strengths outlined above, this study has limitations mainly due to the rarity of GSDIa, which resulted in a small sample size. This limitation consequently reduced the statistical power and hindered the ability to conduct subgroup analyses, including sex-specific evaluations and assessments related to pharmacological treatments and dietary interventions. While the limited cohort size did not allow for a dedicated sex-specific analysis, we performed reanalysis including sex as a covariate for key markers such as PZP and SHBG, confirming that the results remained significant. Nonetheless, we acknowledge the lack of comprehensive sex-specific assessments as a limitation that should be addressed in future studies with larger cohorts. Although detailed stratification based on treatment regimens was not feasible, individual results were interpreted, when possible, considering the clinical management of each patient. For example, while allopurinol—a xanthine oxidase inhibitor commonly used to prevent gout in GSDIa patients—may have confounding effects, elevated serum xanthine levels were observed even in four of six patients not receiving this treatment (P1, P2, P3, P11), suggesting that other factors contribute to these metabolic alterations. Nutritional status represents an additional potential confounder influencing metabolic profiles, warranting cautious interpretation of the results. In particular, the findings regarding SHBG levels in our patients may have been influenced by overnutrition^{64,65}, which is often a consequence of the specific dietary regimens implemented to manage hypoglycemia in GSDIa. Moreover, previous studies have shown that plasma choline levels show minimal variation in healthy individuals⁶⁶, and fasting-mimicking diets have been reported to reduce plasma TMAO levels⁶⁷ supporting the view that the metabolic changes observed in our cohort are primarily disease-related. Nevertheless, these aspects underscore the importance of thoroughly evaluating dietary influences in future research to better define the role of the identified biomarkers. Furthermore, the lack of longitudinal data limits our ability to assess the stability and intra-individual variability of these biomarkers over time, which is crucial for confirming their applicability in ongoing disease monitoring.

Conclusions

The objective of this study was to provide a foundation for the advancement of current research priorities in the domain of hepatic glycogenesis. The investigation was designed to add to the existing body of knowledge concerning metabolic alterations in GSDIa, which are not discernible through conventional monitoring analyses. Complementing the findings of our previous lipidomic analysis¹⁸ the comprehensive assessment provided by this multiomics approach provided new insights into the pivotal role of the liver in the pathophysiology of GSDIa and a detailed assessment of lipid metabolism dysfunction in GSDIa. In this regard, the serum metabolomics findings on choline metabolism support our previous lipidomics data and thus contribute to the conceptualization of a novel working model of choline metabolism impairment in GSDIa. In addition, the positive linear correlation of ALDOB with patient ALT and AST supports further research to investigate its role as a novel potential biomarker of liver injury. Finally, the positive relationship between ALDOB and patient serum uric acid levels supports the potential role of ALDOB in providing substrates for de novo lipogenesis in GSDIa. In conclusion, this study underscores the translational potential of multi-omics approaches to advance the monitoring of GSDIa. The biomarkers identified here offer promising avenues for improving the management and early detection of long-term complications associated with the disease. Further validation in longitudinal cohorts will be essential to confirm their clinical utility and integration into future guidelines.

Methods

Human participants

This study was conducted in accordance with the principles of the Declaration of Helsinki. All studies were performed after informed consent which was obtained from adult participants or the parents of infants.

For patients followed up at the University Medical Center Groningen (Groningen, The Netherlands), the local Medical Ethical Committee indicated that the Medical Research Involving Human Subjects Act was not applicable and official study approval by the Medical Ethical Committee (METC) was not required according to

Parameters	Subjects		<i>p</i> value
	Patients with GSDIa	Healthy controls	Patients with GSDIa versus Healthy controls
Size sample	12	12	–
Age (years)	18 (5–34)	20 (5–31.5)	0.65
Males/females	8/4	8/4	1
Ethnicity	Caucasian	Caucasian	–

Table 1. General characteristics of the study cohorts.

Patients with GSDIa	Age (years)	Gender	G6Pase variation	BMI ^a (kg/m ²)	Dietary regimen	Drugs—Supplements	Clinical features
P1	5	M	p.Arg83Cys p.Arg83Cys	21.0	Frequent feedings; UCCS (3.8 g/kg/day); CNGDF	Vitamin D	Intellectual disability
P2	10	M	p.Arg83Cys p.Arg83Cys	19.7	Frequent feedings UCCS (5.2 g/kg/day)	Vitamin D	–
P3	17	M	p.Trp63Arg p.Arg83Cys	21.4	Frequent feedings Glycosade (3.1 g/kg/day)	–	Previous growth hormone deficiency (rhGH withdrawn 6 months before study enrolment)
P4	25.5	F	p.Trp63Arg p.Arg83Cys	24.4	Frequent feedings Glycosade (3.2 g/kg/day)	Allopurinol Ramipril Fenofibrate	Proteinuria
P5	24	F	p.Arg83Cys p.Arg83Cys	22.5	Frequent feedings; UCCS (3.9 g/kg/day)	ω3 fatty acids	–
P6	34	M	p.Arg83Cys p.Arg83Cys	26.7	Frequent feedings; Glycosade (4.5 g/kg/day)	Allopurinol Carbamazepine	
P7	11	F	p.Arg83Cys p.Arg83Cys	22.2	Frequent feedings; UCCS (4.8 g/kg/day)	Allopurinol Ramipril Vitamin D ω3 fatty acids	Glomerular hyperfiltration
P8	28.5	M	p.Arg83Cys p.Arg83Cys	29.6	Frequent feedings; UCCS (1.5 g/kg/day); CNGDF	Oxybutynin	Urinary incontinence
P9	24	F	p.Arg83Cys p.Arg83Cys	26.3	Frequent feedings; UCCS (4.3 g/kg/day)	Allopurinol Ramipril Vitamin D ω3 fatty acids	Glomerular hyperfiltration
P10	12	M	p.Arg83Cys p.Arg83Cys	19.7	Frequent feedings; CNGDF	Allopurinol Vitamin D ω3 fatty acids	–
P11	10	M	p.Gly270Val p.Gly270Val	21.7	Frequent feedings; UCCS (6.3 g/kg/day)	Vitamin D	–
P12	16	M	p.Gly270Val p.Gly270Val	20.2	Frequent feedings; Glycosade (2.1 g/kg/day) CNGDF	Allopurinol Gemfibrozil	Hepatocarcinoma

Table 2. Clinical features of patients with GSDIa. ^a BMI, body mass index.

protocol n. METc 2019/119. The experimental protocols were approved by the METc at the University Medical Center Groningen (Groningen, The Netherlands), in accordance with the relevant guidelines and regulations included in the n. METc 2019/119 protocol. For patients followed up at the University of Naples Federico II (Naples, Italy), the study protocol was approved by the Ethics Committee of the University of Naples Federico II (Naples, Italy), n. 77/21. The experimental protocols were approved by the Ethics Committee at the University of Naples Federico II (Naples, Italy), in accordance with the relevant guidelines and regulations included in n. 77/21 protocol.

Participants were recruited over a 12 month period and the diagnosis of GSDIa was based on mutation analysis of the G6PC1 gene. The study included 12 patients with GSDIa (8 males and 4 females, median age 16.5 ± 9 years, age range 5–34 years) and 12 age- and sex-matched HC (8 males and 4 females, median age 20.3 ± 9.4 years, age range 5–31.5 years). Among the patients, one was aged < 6 years, five were aged 10–16 years, and six were aged > 17 years. Among the HC, one was aged < 6 years, five were aged 10–16 years, and six were aged > 17 years. Table 1 summarises the general characteristics of the two study cohorts. There was no significant difference between patients and controls in terms of age and sex as calculated by T-test for age and chi-squared test for sex. Details of the clinical characteristics of the patients, including age, sex, genotype, dietary regimen, body mass index, medication and dietary supplements are shown in Table 2. The HC received no dietary or pharmacological treatment.

Serum collection

Blood samples were collected in the pre-prandial state according to each patient's fasting tolerance (3–6 h). To onooxyg bias due to short fasting times, HC were asked to schedule their blood sampling after the same fasting time as their age- and sex-matched GSDIa counterparts. Blood was centrifuged (10 min, 2000 × g at 4 °C) and serum was aliquoted into separate polypropylene tubes which were immediately stored at – 80 °C.

LFQ-proteomics

S-Trap™ micro spin column (Protifi, Hutington, USA) digestion was performed on 50 µg of serum blood according to manufacturer's instructions. Briefly, samples were reduced with 20 mM Tris(2-carboxyethyl) phosphine (TCEP) and alkylated with 50 mM chloroacetamide (CAA) for 15 min at room temperature. Aqueous phosphoric acid was then added to a final concentration of 2.5% following by the addition of S-Trap binding buffer (90% aqueous methanol, 100 mM triethylammonium bicarbonate (TEAB), pH7.1). Mixtures were then loaded on S-Trap columns. Three extra washing steps were performed for thorough SDS elimination. Samples were digested with 2.5 µg of trypsin (Promega) at 47 °C for 1.5 h. After elution, peptides were vacuum dried.

The tryptic peptides were resuspended in 50 µL of 2% acetonitrile (I), 0.1% Formic acid in high-performance liquid chromatography (HPLC)-grade water and an amount of 200 ng was injected on a nanoElute (Bruker Daltonics, Germany) HPLC system coupled to a timsTOF Pro (Bruker Daltonics, Germany) mass spectrometer. HPLC separation (Solvent A: 0.1% formic acid in water; Solvent B: 0.1% formic acid in I) was carried out at 250 nL/min using a packed emitter column (C18, 25 cm × 75 µm 1.6 µm) (Ion Optics, Australia) using a gradient elution (2 to 11% solvent B during 19 min; 11 to 16% during 7 min; 16% to 25% during 4 min; 25% to 80% for 3 min and finally 80% for 7 min to wash the column). Mass-spectrometric data were acquired using the parallel accumulation serial fragmentation (PASEF) acquisition method. The measurements were carried out over the m/z range from 100 to 1700 Th. The range of ion mobilities values from 0.65 to 1.4 V.s/cm² (1/k0). The total cycle time was set to 1.16 s and the number of PASEF MS/MS scans was set to 10.

The obtained data were analyzed using MaxQuant version 2.0.1.0 and searched with Andromeda search engine against the UniProtKB/Swiss-Prot Homo sapiens database (release 02-2021, 20,404 entries). To search parent mass and fragment ions, we set a mass deviation of 3 ppm and 20 ppm respectively. The minimum peptide length was set to 7 amino acids and strict specificity for trypsin cleavage was required, allowing up to two missed cleavage sites. Carbamidomethylation (Cys) was set as fixed modification, whereas oxidation (Met) and N-term acetylation were set as variable modifications. The false discovery rates (FDRs) at the protein and peptide level were set to 1%. Scores were calculated in MaxQuant as described previously. Proteins were quantified according to the MaxQuant label-free algorithm using LFQ intensities; protein quantification was obtained using at least 1 peptide per protein. Match between runs was allowed.

Targeted metabolomics

The serum targeted metabolomic analysis was performed using liquid chromatography–tandem mass spectrometry (LC–MS/MS) based methods as reported by Caterino et al.^{68,69}. Metabolomic analysis was performed according to the protocols of the MxP[®] Quant 500 kit (Biocrates Life Sciences AG, Innsbruck, Austria) on a Triple Quad™ 5500 + System-QTRAP[®] Ready (AB Sciex, Framingham, MA, USA) coupled to a 1260 Infinity II HPLC (Agilent, Santa Clara, CA, USA). The LC–MS/MS based platform was set up to quantify the concentration of the following molecules: amino acids (n = 20), amino acid related (n = 30), biogenic amines (n = 9), carboxylic acids (n = 7), hormones and related (n = 4), indoles and derivatives (n = 4), and alkaloids, amine oxides, cresols, nucleobases and related, vitamins and cofactors (n = 6). Specifically, 10 µL of each serum sample was pipetted onto a 96-well extraction plate containing wells for blanks, PBS, calibrators and quality controls (QC) and dried under a nitrogen stream for 30 min. Quantification was carried out using internal standards (ISTD) and a 7-point calibration curve (Cal 1 to Cal 7). Three human plasma samples spiked with different concentrations of reference analytes (QC1-3) were analyzed as quality control, according to manufacturer's protocol. Each sample was then incubated with 50 µL of 5% phenyl isothiocyanate (PITC) in ethanol/water/pyridine (ratio 1/1/1, v/v/v) for 60 min to derivatise amino acids and biogenic amines and then dried again under a nitrogen stream for 60 min. Metabolites were extracted with 300 µL of 5 mM ammonium acetate in methanol in a shaker (for 30 min, 450 rpm) and eluted into a new 96-well plate by centrifugation.

An aliquot of 150 µL of each extract was diluted with an equal volume of HPLC grade water and the LC–MS/MS measurements were performed to target and quantify metabolites by multiple reaction monitoring (MRM)-based method. Liquid chromatography was performed on a C18 column (Zorbax eclipse XDB 3 × 100 mm, 3.5 µm) using acetonitrile and water with 0.2% formic acid as running solvent. For the LC analysis, the injection volume was 5 µL at an initial flow rate of 0.05 mL/min using the follow gradients: 100% A, 0–0,25 min; 88% A, 0,25–1 min; 82,5% A, 1–3 min; 50% A, 3–4,5 min; 0% A, 4,5–7,5 min for LC1 part coupled with positive ion mode acquisition and 100% A, 0–0,25 min; 75% A, 0,25–0,50 min; 50% A, 0,5–3 min; 25% A, 3–4 min; 0% A, 4,5–7,5 min for LC2 part coupled with negative ion mode acquisition. The autosampler was cooled at 10 °C. The ion source was operated in positive ion mode with the following parameters: spray voltage 55 kV, temperature 450 °C, GS1 20, GS2 40, CUR 30, CAD 8. The ion source was operated in negative ion mode with the following parameters: spray voltage 55 kV, temperature 450 °C, GS1 20, GS2 40, CUR 30, CAD 8.

Data were generated using Analyst software v.1.7.1 (AB Sciex, Framingham, MA, USA) and further processed to calculate metabolite concentrations using MetIDQ™ Oxygen software (Biocrates Life Sciences AG, Innsbruck, Austria).

Proteomics bioinformatic analysis

Bioinformatic analysis and results visualization was performed in R v. 4.3. Reverse proteins, contaminants, and proteins only identified by site were filtered out. Proteins that were not quantified in at least 8 samples of at least

one condition (HC or patient) were also filtered out. The remaining 406 proteins were further analyzed. Data were log₂ scaled. Missing values were imputed by impSeqRob⁷⁰ with alpha parameter equal to 0.95 (less than 5% outlying proteins). Sample-wise normalization was performed by median to obtain the final normalized log₂ (LFQ) data used for differential analysis. Z-scores for heat map visualization were obtained by autoscaling. PCA was performed by a singular value decomposition of the centered data matrix using function prcomp. Differential analysis between HC and patient conditions was performed by SAM method⁷¹ within the R package samr v. 3.0, using t-test and 1000 permutations. Significantly differential proteins were identified with a mixed criterion based on adjusted *p* value (adj. *p*) and fold change (FC), as indicated in specific figure captions. Significant features that had missing (imputed) data were also reanalyzed using sex as a covariate to confirm significance, excluding an unbalance of sex samples between controls and patients. Full data are presented in Supplementary Table 1. Hierarchical clustering with heat map data visualization was performed by package pheatmap v. 1.0.12, using Euclidean distance and complete clustering method. Enrichment analyses were performed using GTEX portal and ShinyGO v. 0.81. Tissue-specific gene expression data were retrieved from the GTEx (Genotype-Tissue Expression) database, which provides transcriptomic profiles (TPM values) across a wide range of human tissues. These data were used to evaluate the tissue distribution of differentially expressed proteins and to generate heat maps of expression patterns. Pathway enrichment analysis was carried out using ShinyGO v. 0.81 to identify significantly overrepresented biological processes.

Metabolomics bioinformatic analysis

Bioinformatic analysis and results visualization was performed in R v. 4.3. Metabolite nomenclature reported in Supplementary information was provided in the targeted metabolomic kit (Biocrates Life Sciences AG). Metabolites that were not quantified in at least 8 samples of at least one condition (HC or patient) were filtered out. The remaining 73 metabolites were further analyzed. Data were log₂ scaled. Missing values were imputed by impSeqRob⁷⁰ with alpha parameter equal to 0.95 (less than 5% outlying proteins). Z-scores for heat map visualization were obtained by autoscaling. The PCA was performed by a singular value decomposition of the centered data matrix using function prcomp. Differential analysis between control and patient conditions was performed by SAM method⁷¹ within the R package samr v. 3.0, using t-test and 1000 permutations. Significantly differential metabolites were identified with a mixed criterion based on adj. *p* and FC, as indicated in specific figure captions. Full data are presented in Supplementary Table 2. Hierarchical clustering with heat map data visualization was performed by function pheatmap v. 1.0.12, using Euclidean distance and complete clustering method.

Multiomics bioinformatic analysis

Multi-omic data analysis was performed integrating proteomic and metabolomic data in terms of z-scores. Pearson's correlation coefficients between features in HC and patient samples were calculated separately, using R package Correlation v. 0.8.4, with a Benjamini–Hochberg *p* value correction for controlling false discovery rate. Result visualization was performed by R package Circlize v. 0.4.16, selecting only significant correlations according to an adjusted *p* value < 0.1. Significant correlations are reported in Supplementary Table 3. Pairs of features whose correlation changed significance between patients and HCs were identified and also reported in Supplementary Table 3. Lost correlations in patients are correlations which are significant in HC (adjusted *p* value < 0.1) and non-significant in patients (adjusted *p* value > 0.1), vice versa holds for gained correlations. The results in Fig. 5 only report the most significant relationships, sub-selected considering an absolute difference of correlation coefficients between patient and HC samples larger than 0.6, and constrained to have at least one significantly differential feature in the lost or gained correlation. Scatter plots were used to display the z-scores of all non-imputed values of pairs of features with significant changes in correlation between HC and patient. Linear models were fitted to HC and patient data separately.

Data availability statement

Data supporting the findings of this study are available in the paper and Supplemental information.

Received: 26 March 2025; Accepted: 6 June 2025

Published online: 01 July 2025

References

- Hannah, W. B. et al. Glycogen storage diseases. *Nat. Rev. Dis. Primers* **9**, 46. <https://doi.org/10.1038/s41572-023-00456-z> (2023).
- Molares-Vila, A., Corbalán-Rivas, A., Carnero-Gregorio, M., González-Cespon, J. L. & Rodríguez-Cerdeira, C. Biomarkers in glycogen storage diseases: An update. *Int. J. Mol. Sci.* **22**, 4381. <https://doi.org/10.3390/ijms22094381> (2021).
- Kanungo, S., Wells, K., Tribett, T. & El-Gharbawy, A. Glycogen metabolism and glycogen storage disorders. *Ann. Transl. Med.* **6**, 474 (2018).
- Chou, J. Y., Jun, H. S. & Mansfield, B. C. Type I glycogen storage diseases: disorders of the glucose-6-phosphatase/glucose-6-phosphate transporter complexes. *J. Inherit. Metab. Dis.* **38**, 511–519 (2015).
- Froissart, R. et al. Glucose-6-phosphatase deficiency. *Orphanet. J. Rare Dis.* **6**, 1–12. <https://doi.org/10.1186/1750-1172-6-27> (2011).
- Derks, T. G. et al. Glycogen storage disease type Ia: Current management options, burden and unmet needs. *Nutrients* **13**, 3828. <https://doi.org/10.3390/nu13113828> (2021).
- Rajas, F., Gautier-Stein, A. & Mithieux, G. Glucose-6 phosphate, a central hub for liver carbohydrate metabolism. *Metabolites* **9**, 282 (2019).
- Kishnani, P. S. et al. Diagnosis and management of glycogen storage disease type I: A practice guideline of the American College of Medical Genetics and Genomics. *Genet. Med.* **16**, 1 (2014).
- Koeberl, D. D. et al. Gene therapy for glycogen storage diseases. *J. Inherit. Metab. Dis.* **47**, 93–118. <https://doi.org/10.1002/jimd.12654> (2024).

10. Petrova, I. O. & Smirnikhina, S. A. Studies on glycogen storage disease type 1a animal models: A brief perspective. *Transgenic Res.* **31**, 593–606. <https://doi.org/10.1007/s11248-022-00325-7> (2022).
11. Rossi, A. et al. A prospective study on continuous glucose monitoring in glycogen storage disease type 1a: Toward glycemic targets. *J. Clin. Endocrinol. Metab.* **107**, e3612–e3623 (2022).
12. Rossi, A. et al. A prospective study on continuous glucose monitoring in glycogen storage disease type 1a: Toward glycemic targets. *J. Clin. Endocrinol. Metab.* **107**, e3612–e3623 (2022).
13. Cho, J. H., Weinstein, D. A. & Lee, Y. M. Emerging roles of autophagy in hepatic tumorigenesis and therapeutic strategies in glycogen storage disease type 1a: A review. *J. Inherit. Metab. Dis.* **44**, 118–128. <https://doi.org/10.1002/jimd.12267> (2021).
14. Melis, D. et al. Progression of renal damage in glycogen storage disease type 1 is associated to hyperlipidemia: A multicenter prospective Italian study. *J. Pediatr.* **166**, 1079–1082 (2015).
15. Aoun, B. et al. Kidney and metabolic phenotypes in glycogen storage disease type-1 patients. *Front. Pediatr.* **8**, 591 (2020).
16. Haring, M. P. D. et al. High childhood serum triglyceride concentrations associate with hepatocellular adenoma development in patients with glycogen storage disease type 1a. *JHEP Rep.* **4**, 100512 (2022).
17. Melis, D. et al. Progression of renal damage in glycogen storage disease type 1 is associated to hyperlipidemia: A multicenter prospective Italian study. *J. Pediatr.* **166**, 1079–1082 (2015).
18. Rossi, A. et al. A specific serum lipid signature characterizes patients with glycogen storage disease type 1a. *J. Lipid Res.* **65**, 100651 (2024).
19. Damska, M., Labrador, E. B., Kuo, C. L. & Weinstein, D. A. Prevention of complications in glycogen storage disease type 1a with optimization of metabolic control. *Pediatr. Diabetes* **18**(5), 327–331 (2017).
20. Niu, L. et al. Defining NASH from a multi-omics systems biology perspective. *J. Clin. Med.* **10**, 4673 (2021).
21. Niu, L. et al. Plasma proteome profiling discovers novel proteins associated with non-alcoholic fatty liver disease. *Mol. Syst. Biol.* **15**(3), e8793 (2019).
22. Govaere, O. et al. A proteo-transcriptomic map of non-alcoholic fatty liver disease signatures. *Nat. Metab.* **5**, 572–578 (2023).
23. Asaka, M., Miyazaki, T., Hollinger, F. B. & Alpert, E. Human aldolase B serum levels: A marker of liver injury. *Hepatology* **4**, 531–535 (1984).
24. Niu, L. et al. Noninvasive proteomic biomarkers for alcohol-related liver disease. *Nat. Med.* **28**, 1277–1287 (2022).
25. Hou, W. et al. Proteomic screening of plasma identifies potential noninvasive biomarkers associated with significant/advanced fibrosis in patients with nonalcoholic fatty liver disease. *Biosci. Rep.* **40**, BSR20190395 (2020).
26. Veyel, D. et al. Biomarker discovery for chronic liver diseases by multi-omics—a preclinical case study. *Sci. Rep.* **10**, 1314 (2020).
27. Stocks, B. et al. Integrated liver and plasma proteomics in obese mice reveals complex metabolic regulation. *Mol. Cell. Proteom.* **21**, 100207 (2022).
28. Lei, Y. et al. Hepatic carbohydrate response element binding protein activation limits nonalcoholic fatty liver disease development in a mouse model for glycogen storage disease type 1a. *Hepatology* **72**, 1638 (2020).
29. Cangelosi, D. et al. A proteomic analysis of GSD-1a in mouse livers: Evidence for metabolic reprogramming, inflammation, and macrophage polarization. *J. Proteome Res.* **18**, 2965–2978 (2019).
30. Ter Horst, K. W. & Serlie, M. J. Fructose consumption, lipogenesis, and non-alcoholic fatty liver disease. *Nutrients* **9**, 981. <https://doi.org/10.3390/nu9090981> (2017).
31. Simons, P. I. et al. Serum sex hormone-binding globulin levels are reduced and inversely associated with intrahepatic lipid content and saturated fatty acid fraction in adult patients with glycogen storage disease type 1a. *J. Endocrinol. Invest.* **45**, 1227–1234 (2022).
32. Wang, X. et al. Serum SHBG is associated with the development and regression of nonalcoholic fatty liver disease: A prospective study. *J. Clin. Endocrinol. Metab.* **105**, e791–804 (2020).
33. Kim, D., Manikat, R., Cholankeri, G. & Ahmed, A. Endogenous sex hormones and nonalcoholic fatty liver disease in <sc>US</sc> adults. *Liver Int.* **44**, 460–471 (2024).
34. Bourebaba, N., Ngo, T., Śmieszek, A., Bourebaba, L. & Marycz, K. Sex hormone binding globulin as a potential drug candidate for liver-related metabolic disorders treatment. *Biomed. Pharmacother.* **153**, 113261 (2022).
35. Simó, R., Sáez-López, C., Barbosa-Desongles, A., Hernández, C. & Selva, D. M. Novel insights in SHBG regulation and clinical implications. *Trends Endocrinol. Metab.* **26**, 376–383 (2015).
36. Rossi, A. et al. Endocrine involvement in hepatic glycogen storage diseases: Pathophysiology and implications for care. *Rev. Endocr. Metab. Disord.* **25**, 707–725 (2024).
37. Deswal, R., Yadav, A. & Dang, A. S. Sex hormone binding globulin—an important biomarker for predicting PCOS risk: A systematic review and meta-analysis. *Syst. Biol. Reprod. Med.* **64**, 12 (2018).
38. Wang, C. et al. Mendelian randomization analyses for PCOS: Evidence, opportunities, and challenges. *Trends Genet.* **38**, 468–482. <https://doi.org/10.1016/j.tig.2022.01.005> (2022).
39. Rossi, A. et al. Imbalanced cortisol concentrations in glycogen storage disease type 1: Evidence for a possible link between endocrine regulation and metabolic derangement. *Orphanet. J. Rare Dis.* **15**, 1 (2020).
40. Liu, M. et al. Big data-based identification of multi-gene prognostic signatures in liver cancer. *Front. Oncol.* **10**, 847 (2020).
41. Zhang, Y., Zhang, J., Chen, X. & Yang, Z. Polymeric immunoglobulin receptor (Pigr) exerts oncogenic functions via activating ribosome pathway in hepatocellular carcinoma. *Int. J. Med. Sci.* **18**, 364 (2021).
42. Ai, J. et al. The role of polymeric immunoglobulin receptor in inflammation-induced tumor metastasis of human hepatocellular carcinoma. *J. Natl. Cancer Inst.* **103**, 1696 (2011).
43. Yao, Q. et al. Osteoarthritis: Pathogenic signaling pathways and therapeutic targets. *Signal Transduct. Targeted Therapy* **8**, 56. <https://doi.org/10.1038/s41392-023-01330-w> (2023).
44. Dituri, F. et al. Proteoglycan-4 is correlated with longer survival in HCC patients and enhances sorafenib and regorafenib effectiveness via CD44 in vitro. *Cell Death Dis.* **11**, 984 (2020).
45. Su, L., Zhang, G. & Kong, X. Prognostic significance of pregnancy zone protein and its correlation with immune infiltrates in hepatocellular carcinoma. *Cancer Manag. Res.* **12**, 9883–9891 (2020).
46. Ke, H. et al. Serum protein biomarkers for HCC risk prediction in HIV/HBV co-infected people: a clinical proteomic study using mass spectrometry. *Front. Immunol.* **10**, 1282469 (2023).
47. Xu, Y. et al. Hepatocyte-specific expression of human carboxylesterase 1 attenuates diet-induced steatohepatitis and hyperlipidemia in mice. *Hepatology Commun.* **4**, 527–539 (2020).
48. Perdomo, G. et al. A role of apolipoprotein D in triglyceride metabolism. *J. Lipid Res.* **51**, 1298–1311 (2010).
49. Jiménez-Palmares, M., Cózar-Castellano, I., Ganfornina, M. D., Sánchez, D. & Perdomo, G. Genetic deficiency of apolipoprotein D in the mouse is associated with nonfasting hypertriglyceridemia and hyperinsulinemia. *Metabolism* **60**, 1767–1774 (2011).
50. Bandsma, R. H. et al. Increased de novo lipogenesis and delayed conversion of large VLDL into intermediate density lipoprotein particles contribute to hyperlipidemia in glycogen storage disease type 1a. *Pediatr. Res.* **63**, 702–707 (2008).
51. Hoogerland, J. A. et al. Impaired very-low-density lipoprotein catabolism links hypoglycemia to hypertriglyceridemia in glycogen storage disease type 1a. *J. Inherit. Metab. Dis.* **44**, 879–892 (2021).
52. El-Gharbawy, A. et al. Beyond predicting diagnosis: Is there a role for measuring biotinidase activity in liver glycogen storage diseases?. *Mol. Genet. Metab. Rep.* **31**, 100856 (2022).
53. Forny, P., Burda, P., Bode, P. & Rohrbach, M. Is serum biotinidase enzyme activity a potential marker of perturbed glucose and lipid metabolism?. *JIMD Rep.* **57**, 58–66 (2021).

54. Rossi, A. et al. Insulin-resistance in glycogen storage disease type Ia: linking carbohydrates and mitochondria?. *J. Inherit. Metab. Dis.* **41**, 985–995 (2018).
55. Lindblom, P. et al. Isoforms of alanine aminotransferases in human tissues and serum—differential tissue expression using novel antibodies. *Arch. Biochem. Biophys.* **466**, 66–77 (2007).
56. Mathis, T. et al. Untargeted plasma metabolomics identifies broad metabolic perturbations in glycogen storage disease type I. *J. Inherit. Metab. Dis.* **45**, 235–247 (2022).
57. Farah, B. L. et al. Hepatic mitochondrial dysfunction is a feature of Glycogen storage disease type Ia (GSDIa). *Sci. Rep.* **7**, 44408 (2017).
58. Olthof, M. R., Brink, E. J., Katan, M. B. & Verhoef, P. Choline supplemented as phosphatidylcholine decreases fasting and postmethionine-loading plasma homocysteine concentrations in healthy men. *Am. J. Clin. Nutr.* **82**, 111–117 (2005).
59. Cole, L. K., Vance, J. E. & Vance, D. E. Phosphatidylcholine biosynthesis and lipoprotein metabolism. *Biochim. Biophys. Acta BBA-Mol. Cell Biol. Lipids* **1821**, 754–761 (2012).
60. Taniguchi, M. & Okazaki, T. Ceramide/sphingomyelin rheostat regulated by sphingomyelin synthases and chronic diseases in murine models. *J. Lipid Atherosclerosis* **9**(3), 380. <https://doi.org/10.12997/jla.2020.9.3.380> (2020).
61. Inazu, M. Functional expression of choline transporters in the blood–brain barrier. *Nutrients* **11**(10), 2265 (2019).
62. Mailloux, R. J. et al. Choline and dimethylglycine produce superoxide/hydrogen peroxide from the electron transport chain in liver mitochondria. *FEBS Lett.* **590**, 4318–4328 (2016).
63. Wang, Y. et al. Altered gut microbiota and microbial metabolism in children with hepatic glycogen storage disease: a case-control study. *Transl. Pediatr.* **12**, 572 (2023).
64. Singh, P. et al. Overfeeding-induced weight gain elicits decreases in sex hormone-binding globulin in healthy males—Implications for body fat distribution. *Physiol. Rep.* **9**(23), e15127 (2021).
65. Pritchard, J. et al. Plasma adrenal, gonadal, and conjugated steroids before and after long term overfeeding in identical twins. *J. Clin. Endocrinol. Metab.* **83**, 3277–3284 (1998).
66. Wiedeman, A. M. et al. Variations in plasma choline and metabolite concentrations in healthy adults. *Clin. Biochem.* **60**, 77 (2018).
67. Videja, M. et al. Fasting-mimicking diet reduces trimethylamine N-oxide levels and improves serum biochemical parameters in healthy volunteers. *Nutrients* **14**, 1093 (2022).
68. Caterino, M. et al. The serum metabolome of moderate and severe covid-19 patients reflects possible liver alterations involving carbon and nitrogen metabolism. *Int. J. Mol. Sci.* **22**, 9548 (2021).
69. Caterino, M. et al. Dysregulation of lipid metabolism and pathological inflammation in patients with COVID-19. *Sci. Rep.* **11**, 2941 (2021).
70. Vanden Branden, K. & Verboven, S. Robust data imputation. *Comput. Biol. Chem.* **33**, 7–13 (2009).
71. Tusher, V. G., Tibshirani, R. & Chu, G. Significance analysis of microarrays applied to the ionizing radiation response. *Proc. Natl. Acad. Sci.* **98**, 5116–5121 (2001).

Acknowledgements

This work was funded by PRIN (Progetti di Ricerca di Rilevante Interesse Nazionale) [Grant number: Prot. 2022H77XMH; title: ‘Identification of new disease specific omic signatures and therapeutic targets for Glycogen storage disease type Ia’] to Margherita Ruoppolo, Daniela Melis, Camilla Luni. Funded by the European Union—Next Generation EU.

Author contributions

Conceptualization: MR, MC, FP, CL, DM, AR, MHO, TGJD; Formal analysis: RA, CL, MC, FP; Writing-original draft: FP, MHO; Funding acquisition: MR, CL, DM, GP; Supervision: MR, MC, CL, DM, GP, PS; Methodology: MC, CL, FP, RF, CR; Software: RA, CL, MC, FP; Resources: MR, MC, CL, AR, DM; Visualization: RA, CL, FP; Writing—review & editing: CL, MR, MC, FP, MHO.

Declarations

Competing interests

The authors declare no competing interests.

Additional information

Supplementary Information The online version contains supplementary material available at <https://doi.org/10.1038/s41598-025-06272-7>.

Correspondence and requests for materials should be addressed to M.C. or M.R.

Reprints and permissions information is available at www.nature.com/reprints.

Publisher’s note Springer Nature remains neutral with regard to jurisdictional claims in published maps and institutional affiliations.

Open Access This article is licensed under a Creative Commons Attribution-NonCommercial-NoDerivatives 4.0 International License, which permits any non-commercial use, sharing, distribution and reproduction in any medium or format, as long as you give appropriate credit to the original author(s) and the source, provide a link to the Creative Commons licence, and indicate if you modified the licensed material. You do not have permission under this licence to share adapted material derived from this article or parts of it. The images or other third party material in this article are included in the article’s Creative Commons licence, unless indicated otherwise in a credit line to the material. If material is not included in the article’s Creative Commons licence and your intended use is not permitted by statutory regulation or exceeds the permitted use, you will need to obtain permission directly from the copyright holder. To view a copy of this licence, visit <http://creativecommons.org/licenses/by-nc-nd/4.0/>.

© The Author(s) 2025